Vietnam Journal of Science and Technology ***63*** *(6) (2025) 1160-1173*

doi:10.15625/2525-2518/19366

Silver nanoparticles synthesized using *S. nervosum* leaf extract, and their antibacterial and antifungal activity

Cong Hong Hanh[1, *], Pham Sy Hieu[1], Nguyen Hong Nhung[1], Tran Que Chi[1], Tran Thi Huong[1], Pham Duy Khanh[1], Pham Thi Gam[2], Nguyen Van Phuong[3], Phan Thi Thanh Nga[4], Hoang Hien Y[5, 6], Dao My Uyen[5, 6], Hoang Anh Son[1, *]

[1]*Institute of Materials Science, Vietnam Academy of Science and Technology, 18 Hoang Quoc Viet, Nghia Do ward, Ha Noi, Viet Nam*

[2]*Faculty of Pharmacy, Ha Noi University of Business and Technology, Vinh Tuy ward, Ha Noi, Viet Nam*

[3]*University of Science and Technology of Hanoi, Vietnam Academy of Science and Technology, 18 Hoang Quoc Viet, Nghia Do ward, Ha Noi, Viet Nam*

[4]*Faculty of Chemical Engineering, Ho Chi Minh City University of Technology, 268 Ly Thuong Kiet, Dien Hong ward, Ho Chi Minh, Viet Nam*

[5]*Center for Advanced Chemistry, Institute of Research & Development, Duy Tan University, Da Nang, Viet Nam*

[6]*Faculty of Natural Sciences, Duy Tan University, Da Nang, Viet Nam*

[*]Emails: *1. hanhch@ims.vast.ac.vn, 2. sonha@ims.vast.ac.vn*

Received: 7 November 2023; Accepted for publication: 13 October 2025

Abstract. In this study, the green synthesis of silver nanoparticles (AgNPs) was performed using S.nervosum leaf extract, and their physicochemical characterization was also studied. The characteristic surface plasmon resonance peak observed in the visible region at 435 nm is consistent with previous reports of silver nanoparticle formation. The synthesized AgNPs were also characterized by SEM, TEM, XRD, and FTIR, which revealed their nearly spherical shape, with a diameter mainly in the 10 - 30 nm range. The antimicrobial activity of AgNPs was studied using the agar well diffusion method on four clinically significant pathogenic microorganisms (*P. aeruginosa* ATCC 27853; *E. coli* ATCC 35218, *S. aureus* ATCC 12493; *S. aureus* Mastitis isolate). The results showed that the green-synthesized AgNPs exhibited antimicrobial activity at most studied concentrations, including the antibacterial effect against the S. Aureus (Mastitis isolate) strain, which was found to be resistant to Tetracycline at 100 µg/L. The antifungal activity of these nanoparticles was also studied on *Colletotrichum gloeopsoriodes* by colony formation assay. The green synthesis of AgNPs was successfully conducted for the first time using the aqueous extract of S. *nervosum*. The results of this study indicate that the silver nanoparticles have potential applications as antibacterial and antifungal agents.

Keywords: Green synthesis, AgNPs, S. *nervosum*, antibacterial activity, antifungal activity.

Classification numbers: 3.7.3

1. INTRODUCTION

In recent years, nanotechnology associated with metal nanoparticles has garnered significant attention in the sciences and is widely applied in various fields, including physics, chemistry, and biology [1, 2]. Metal nanoparticles possess unique properties due to their excellent physicochemical properties, including electrical and thermal conductivity, as well as a high surface-to-volume ratio, which are essential for applications in catalysis, biomedicine, energy, environmental protection, electronics, and optoelectronics [3 - 7]. Among these metals, silver nanoparticles (AgNPs) have garnered more interest due to their remarkable properties, including good electrical conductivity, chemical stability, catalytic activity, and antibacterial, antiviral, and antifungal activities [8 - 13]. Various approaches have been developed to synthesize AgNPs, including chemical, physical, and biological methods [14]. Generally, conventional physical and chemical methods are used to manufacture nanoparticles with high stability and controlled size [15]. Unfortunately, their high cost, low reaction yield, hazardous nature, and high energy consumption are significant drawbacks [16, 17].

In contrast, the synthesis of metal nanoparticles by biological or green synthesis methods has recently received considerable attention due to their potential for less toxicity, cost-effectiveness, and feasibility [18,19]. They utilize biological resources and eco-friendly materials, such as microorganisms, fungi, and plant extracts, which can potentially reduce metal ions [20]. The synthesis of nanoparticles from microorganisms and fungi enables the control and regulation of size and morphology, as well as the use of low residual amounts of reducing agents. However, highly sterile conditions, culture contamination, and long reaction times are significant challenges for the synthesis [21]. Plant phytochemicals include alkaloids, flavonoids, glycosides, polysaccharides, terpenoids, and tannins, which are suggested to reduce agents and stabilize AgNPs [22].

Plant S. *nervosum* belongs to the Syzygium Genus, Myrtaceae family. They are cultivated in many provinces of Viet Nam and other Southeast Asian countries. The leaf and bud extracts of S.nervosum are widely used in traditional medicine, particularly for treating influenza, skin diseases, and digestive conditions. The leaf extract of *S. nervosum* contains polyphenols, flavonoids, vitamins, and minerals, and has been shown to exhibit anticancer, antidiabetic, antiobesity, antioxidant, antiviral, anti-inflammatory, and other bioactivities [23]. The high polyphenol content in the leaf extract can be effectively utilized as a reducing agent for synthesizing nanomaterials [24].

Silver nanoparticles have extensive applications in the fields of medicine and healthcare due to their pronounced antibacterial and antifungal properties [25]. The escalating concern of antibiotic resistance poses a significant threat to global health, particularly in developing nations like Viet Nam, where antibiotic usage lacks stringent control measures. The promising prospect of AgNPs as a viable alternative to antibiotics has garnered considerable attention. The antibacterial efficacy of AgNPs operates through a multifaceted mechanism, targeting microorganisms across diverse structures simultaneously, endowing them with the capability to combat a broad spectrum of bacterial strains [26]. *Staphylococcus aureus* is one of the most frequently identified local pathogens, as well as the type of bacteria causing the major types of resistant infections. Infections caused by antibiotic-resistant strains of *S. aureus have become a serious global* problem. They cause invasive infections, inflammation in many tissues, blood infections, and even life-threatening infections.

In this study, we utilized S.nervosum leaf extract to synthesize silver nanoparticles, aiming to combine the antibacterial properties of the silver nanoparticles with the pharmacological effects of the leaves to obtain a promising, environmentally friendly new product. In addition, the antibacterial activity test against Gram-negative bacteria (*Escherichia coli*; ATCC 35218)

and Gram-positive bacteria (Staphylococcus aureus; ATCC 12493 and an antibiotic-resistant S. aureus strain) was also performed, yielding positive results.

2. MATERIALS AND METHODS

2.1. Materials

The S. *nervosum* used in this work was fresh and green, purchased from a supermarket in Vietnam. Silver Nitrate ($AgNO_3$, purity of 99 %, VWR Chemical), Polyvinylpyrrolidone (PVP, average molecular weight 1300000, Sigma-Aldrich). Deionized Water made in our lab was used in this experiment. Other reagents and chemicals are of analytical purity and were used without further purification.

2.2. Methods

Preparation of *S. nervosum* leaf aqueous extract: Freshly harvested *S. nervosum* leaves are washed with distilled Water and dried for 1 hour. Afterward, 20 g of chopped *S. nervosum leaves were immersed in 450 mL of deionized Water, placed* on a hot plate, and allowed to boil for 5 min. The leaf extract solution was obtained after three rounds of filtration and was ready for the next step of the experiment.

Synthesis of AgNPs using S.*nervosum* leaf aqueous extract: The AgNPs were prepared by reducing an $AgNO_3$ solution (1 mM) to 1 mM in the presence of the *S. nervosum* leaf extract. The mixture of 1 ml polyvinylpyrrolidone (PVP) 10 % and 10 ml of $AgNO_3$ with different concentrations (0.01, 0.02 0.04, 0.06, 0.08M) was added to 40 ml of *S. nervosum* aqueous leaf extract at room temperature, and solutions were kept on a magnetic stirrer for vigorous mixing to optimize the reduction of $AgNO_3$ by the *S. nervosum* leaf extract.

Characterization of AgNPs: The formation and optical properties of AgNPs synthesized by *S. nervosum* leaf extract were measured by the UV-Vis absorbance spectrophotometer in the visible region from 350 to 750 nm (Picodrop spectrometer P200, UK). The size and distribution of Ag nanoparticles were measured by Dynamic Light Scattering (DLS) (Zetasizer Nano-ZS, Malvern). FTIR analysis was performed to identify the biomolecules and functional groups present on the synthesized nanoparticles. The crystalline phase of the synthesized AgNPs was examined with an XRD analyzer to confirm the crystallinity of Ag nanoparticles. The surface morphology and microstructure of AgNPs were examined using field-emission Scanning Electron Microscopy (FESEM) (Hitachi S4800) and High-Resolution Transmission Electron Microscopy (HRTEM) and selected area electron diffraction (SAED) images were taken on a JEOL JEM-2100.

Antibacterial assay: The antibacterial activity of AgNPs was assessed by agar well diffusion test [27, 28] against two Gram-negative bacteria (*Escherichia coli*; ATCC 35218, *Pseudomonas aeruginosa*; ATCC 27853) and two Gram-positive bacteria (*Staphylococcus aureus*; ATCC 12493 and *S. aureus*; local isolate from mastitis-infected cows). The bacterial stock cultures were streaked on the assay plate (90 × 15 mm in dimensions) containing Tryptic Soy Agar (TSA, BK046HA, Biokar Diagnostic) and incubated overnight at 37 °C. One colony of each overnight culture was used to prepare bacterial suspension by shaking in 20 mL of Tryptic Soy Broth (TSB, BK046HA, Biokar Diagnostic) for 4 h at 37 °C and 160 rpm. The bacterial suspension was made in a sterile saline solution (0.85 %) and adjusted to a 0.5 McFarland standard (1.5 × 108 CFU/mL). Sterile swabs were used to inoculate TSA plates, where the tip of

the swab was immersed in the bacterial suspension, and then the wet swab was uniformly passed over the entire surface of the plate. Then, nine holes with a diameter of 6 mm were aseptically punched using a sterile cork borer. Afterward, 20 µL of the AgNP solutions at various concentrations (200, 100, 50, and 25 ppm) were introduced into the corresponding wells. The same volume of sterile Water and standard antibiotics was used as negative and positive controls, respectively. Ciprofloxacin (25 µg/l) was used as the positive control for P. aeruginosa, and Tetracycline (100 µg/l) was used for other strains. The agar plates were incubated at 37 °C for 24 h. Then, the diameter of the inhibition zone was measured in millimeters, and the antimicrobial effect of AgNP solutions was analyzed. The experiment was carried out in triplicate.

Figure 1. Graphic representation of AgNPs synthesis.

Antifungal activity of AgNPs by disk diffusion method: The antifungal activity of synthesized AgNPs was investigated by measuring the diameter of the fungal colonies that were growing [29]. Following the preparation of the culture medium for pathogenic fungi, specifically Potato Dextrose Agar (PDA), which included incorporating the examined sample, the fungus plate was subsequently subcultured after three days. A well was created in the center of the petri dish (diameter = 8 mm) to transfer the fungal sample. Subsequently, the plates were incubated within a hermetically sealed enclosure maintained at room temperature. The sample was monitored for five days, during which the diameter of the fungal growth region (in millimeters) was measured. The fungal strain employed in the experiment is Colletotrichum gloeopsoriodes, a pathogenic fungus responsible for inducing fruit rot in chili peppers (*Capsicum annum* L.). The AgNPs were used at a concentration of 200 ppm, and the PDA medium underwent autoclaving at a temperature of 121°C for 15 minutes, followed by subsequent cooling to a temperature of 60°C. Subsequently, a volume of 1 mL of the sample containing AgNPs dispersed in distilled Water was introduced into 20 mL of growth medium, resulting in the formation of a homogeneous mixture. This combination was then carefully transferred into a Petri plate and maintained at room temperature to facilitate the solidification of the agar medium. The aforementioned procedure was executed within a controlled environment, specifically an incubator, in order to mitigate the risk of microbial contamination. The efficacy of the investigated AgNPs will be assessed by measuring their antifungal activity, specifically the suppression rate of mycelium growth. This parameter was determined using the following equation [30]:

$$\boldsymbol{Inhibition\ rate}\ (\%) = \frac{(\boldsymbol{D-d})}{\boldsymbol{D}} \times \mathbf{100} \quad (1)$$

where: D (mm) control colony diameter; d: treated colony diameter (AgNPs).

3. RESULTS AND DISCUSSION

3.1. The UV-Vis spectrum

UV-Vis absorption spectrometry was performed to confirm the synthesis of silver nanoparticles, with spectra recorded over the range of 350 - 750 nm (Figure 2). The distance between the particle size and its dielectric constant is mainly dependent on the size and shape of the particles, which causes a change in surface plasmon resonance [31]. A distinct SPR peak at 435 nm was observed, consistent with characteristic signatures reported for AgNPs, while no corresponding peaks appeared in the spectra of the $AgNO_3$ solution or the S. nervosum leaf extract, confirming the reduction of Ag^+ to metallic Ag^0 nanoparticles. The resulting colloidal AgNPs exhibit good stability, likely due to the capping and stabilizing effects of biomolecules present in the extract. Moreover, varying the $AgNO_3$ precursor concentration (0.01 - 0.08 M) revealed a proportional increase in SPR peak intensity, reflecting the enhanced formation of AgNPs at higher precursor levels. SPR bands consistently appeared within the typical 400 - 450 nm region for silver nanoparticles [32]. The maximum intensity of the SPR peak was observed at an $AgNO_3$ concentration of 0.08M, so the number of AgNPs produced is the highest. Therefore, 0.08M of $AgNO_3$ was considered ideal for further studies.

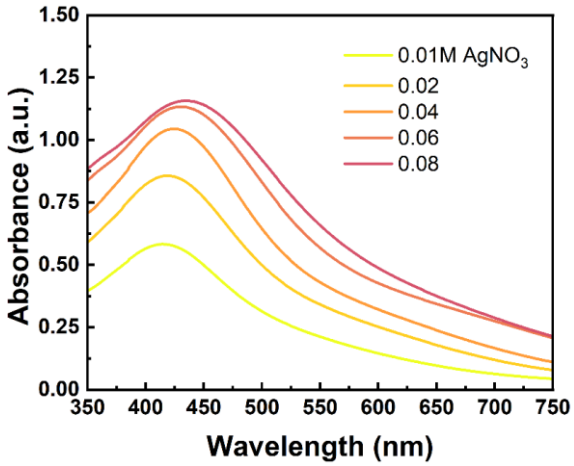

Figure 2. The UV-Vis spectra of synthesized silver nanoparticles at different $AgNO_3$ concentrations.

3.2. The Dynamic Light Scattering (DLS)

DLS is the most versatile and valuable technical method for in situ measurement of nanoparticle size and size distribution in liquids. In our present work, DLS measurements demonstrate the presence of AgNPs synthesized using a green method from S. *nervosum* leaf extract. Figure 3 shows that the successfully synthesized AgNPs have a particle size of approximately 5 to 30 nm for AgNO3 concentrations ranging from 0.01 to 0.08 M, respectively. Particle size measurements by DLS can be larger than those by SEM and TEM due to the presence of organic compounds in the sample. The PDI values of the samples ranged from 0.3 to 0.4, which falls within the range of 0-1, where 0 refers to monodisperse, and 1 refers to polydisperse [33, 34]. It has been reported that samples with PDI values lower than 0.3 would exist in monodisperse form. This result indicates that the synthesized AgNPs were mostly in a monodisperse phase, and the aggregation observed here is attributed to compounds in the plant extract [34].

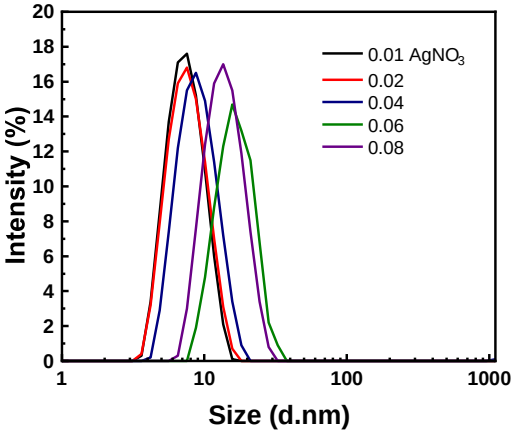

Figure 3. Size distribution of AgNPs by DLS.

The zeta potential values can determine the stability of the AgNPs. High zetapotential causes a strong repulsive force among the particles, thus preventing them from aggregating [34]. In our study, the sample of 0.08 M $AgNO_3$ has the highest zeta potential value (-29.5 mV) (Table 1), which reinforces its ideal status.

Table 1. Zetapotential values of synthesized AgNPs.

Samples	Zeta potential (mV)
$AgNO_3$ 0.01 M	-16.7
$AgNO_3$ 0.02 M	-17.1
$AgNO_3$ 0.04 M	-22.8
$AgNO_3$ 0.06 M	-26.3
$AgNO_3$ 0.08 M	-29.5

3.3. The FTIR spectra

FTIR spectra were recorded to identify functional groups that may be bound to biomolecules or phytochemicals, whose extracts are significant for reducing manufactured AgNPs, as shown in Figure 4. The strong absorption peak at 3380 cm^{-1} is attributed to the presence of the (–OH) group in the phenolic compounds. The absorption bands at 2931 cm^{-1} indicate the presence of alkyl (–CH) stretch (sp^3). Additionally, the weak peak at 1723 cm^{-1} represents the frequency form of the (C—O) of the ester group, while a peak at 1617 cm^{-1} presents the (C—O) of the primary amide group. The δs of the methylene ($–CH_2$) group are identified at the sharp peak at 1425 cm^{-1}. Moreover, the absorption bands at 1293 cm^{-1} and 1028 cm^{-1} are attributable to the vibrational frequencies of the ($–CH_3$) group. The absorption band at 1040 cm^{-1} represents the vibration of the (C—O) group. Finally, the absorption bands at 735 cm^{-1} and 646 cm^{-1} are vibrations of the ($–CH_2$) and (C=C) groups, respectively [35]. These specific functional groups are consistent with the standard eugenol signal, confirming the presence of eugenol in the S.*nervosum* leaf extract. The FTIR spectra suggested that the S.*nervosum* leaf extract successfully synthesizes AgNPs. During heat treatment at 100 °C, the absorption of the (–OH) group at 3380 cm^{-1} is significantly reduced, allowing for preservation, storage, and preparation for further experiments.

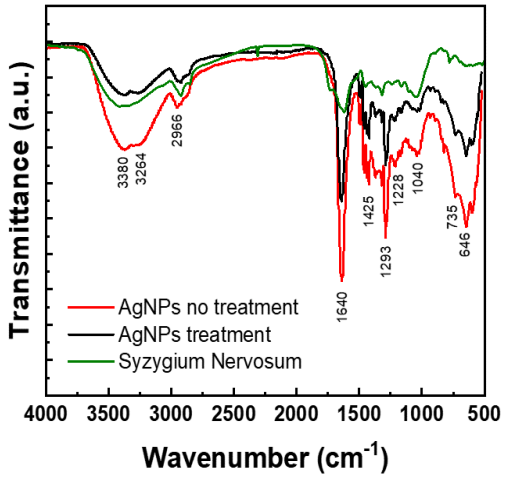

Figure 4. The FTIR spectra of AgNPs treatment (heat treatment at 100 ºC), AgNPs no treatment, and *Syzygium Nervosum*.

3.4. Characterization of AgNPs

Figure 5 shows the XRD pattern of the AgNPs synthesized by S.*nervosum* leaf extract. Sharp and intense peaks describe the highly crystalline silver nanoparticles synthesized. The peaks at 2θ: 37.8° (111), 44.9° (200), and 64.8° (220) indicate the formation of a face-centered cubic center (FCC) structure of AgNPs (JCPDS No.4.783) [32]. The mean crystallite size was calculated by the value of a strong peak at 37.8° using the Scherrer formula given by Equation 2:

$$D = \frac{k\lambda}{\beta cos\theta} \quad (2)$$

where k is the shape factor, which is equal to 0.9, λ is the wavelength of X-ray (CuKα = 0.15406 nm), β is the full width at half maximum (FWHM) of the diffraction peak, and θ is the peak position. The average crystallite size estimated was approximately 15 nm. The morphology of the AgNPs synthesized was analyzed using SEM and TEM, as shown in Figure 6.

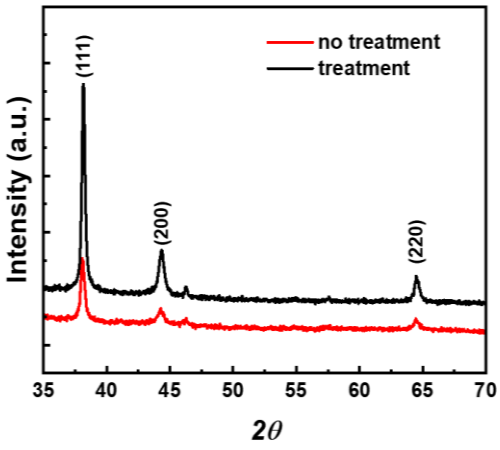

Figure 5. The XRD pattern of AgNPs treatment (heat treatment at 100 ºC) and AgNPs no treatment.

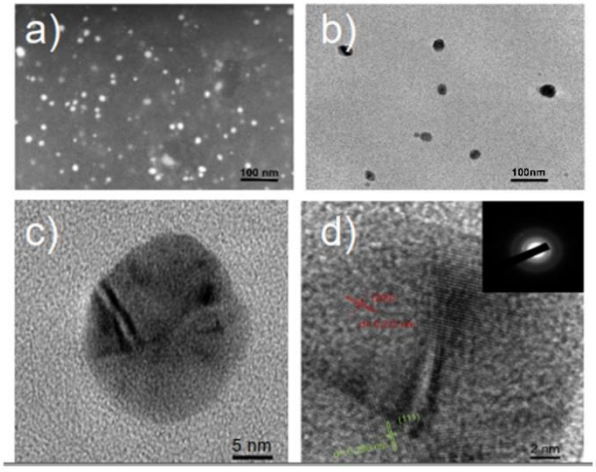

Figure 6. The morphology of synthesized silver nanoparticles: a) SEM image b) TEM image, c) and d) HR-TEM images.

In Figure 6a, we observed that silver nanoparticles synthesized by the plant leaf extract have a high yield and uniformity. The nanoparticles are nearly spherical, with diameters mainly in the 10 - 30 nm range, consistent with the results of the TEM analysis shown in Figure 6b. The HR-TEM image is presented in Figure 6c, with a particle size of 20 nm, which is consistent with the result of SEM (Figure 6a). The nanoparticles present as a pentagonal nanostructure due to growth in the plane (111). The SAED (Figure 6d) image of AgNPs synthesized is consistent with the previous X-ray diffraction results on the crystal structure of the synthesized AgNPs and presence in three planes (111), (200), and (220).

3.5. The antibacterial

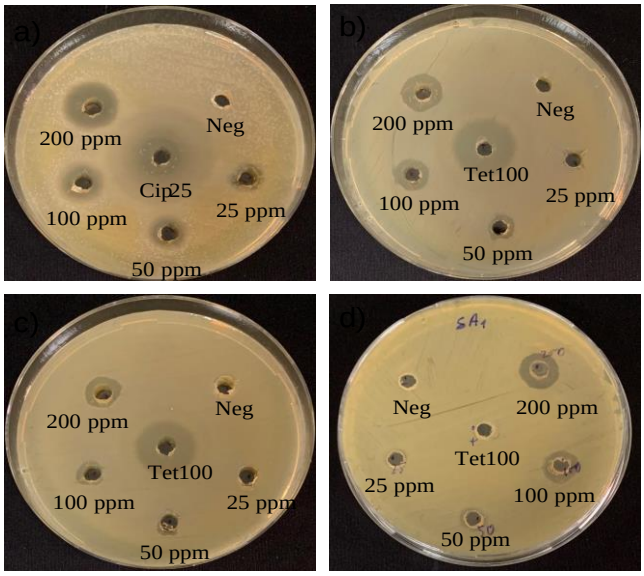

Figure 7. Antibacterial activity of green synthesized AgNPs against: a) *P.aeruginosa* ATCC 27853, b) *E. coli* ATCC 35218, c) *S. aureus* ATCC 12493, and d) *S. aureus* (Mastitis isolate).

Table 2. Antibacterial activity of AgNPs against some bacterial strains.

[AgNPs] (mg/l)	Zone of Inhibition (mm)			
	P. aeruginosa ATCC27853	*E. coli* ATCC 35218	*S. aureus* ATC 12493	*S. aureus* Mastitis isolate
Pos. control	31.5 ± 0.3	18.94 ± 0.4	18.8 ± 0.5	NI
Neg. control	NI	NI	NI	NI
200	16.3 ± 0.3	11.8 ± 0.3	11.0 ± 0.4	11.8 ± 0.4
100	13.2 ± 0.6	10.4 ± 1.1	9.5 ± 0.4	10.1 ± 0.4
50	10.2 ± 0.7	8.1 ± 0.2	7.8 ± 0.1	8.0 ± 0.1
25	9.1 ± 0.5	6.4 ± 0.3	NI	6.4 ± 0.3

Table 3. Antibacterial effect of AgNPs against the strain of *S.aureus* or MRSA.

No	Properties of AgNPs	The synthetic method	Antibacterial activity	Ref
1	Nanometric size (up to 100 nm), spherical, irregular morphologies and a polydispersed character.	Green synthesis, using extracts of neem, onion and tomato	The addition of green-synthesized AgNPs to antibiotics has increased their antimicrobial activity against SA microorganisms.	[36]
2	Levofloxacin-conjugated AgNPs.	Silver nanoparticles (AgNPs) conjugated with Levofloxacin	Levo–AgNPs appeared to have high antimicrobial activity against *S.aureus* (ATCC 29213) and MRSA strains compared to free Levofloxacin.	[37]
3	AgNPs with spherical shapes and sizes ranged from 8.55 to 20.3 nm	Synthesis by using soluble starch	The mean values of MIC and MBC of AgNPs against MRSA were 8.125 ± 0.19 and 13.125 ± 0.78 µg/mL, respectively.	[38]
4	AgNPs with a mean size of 18.34 nm		AgNPs at a concentration of 4 μg/ml completely inhibited the growth of *S. aureus* PTCC1431.	[39]
5	AgNP encapsulating pNIPAM and pNIPAM-NH_2 polymeric nanoparticles	Silver nanoparticles encapsulated in poly-n-isopropylacrylamide-based polymeric nanoparticles	Both AgNP-pNIPAM/ pNIPAM-NH_2 nanoparticles showed antimicrobial effects against *S.aureus* (which were lower than those for *E.coli*.)	[40]

The antimicrobial activity of AgNPs was studied using the agar well diffusion method on four clinically significant pathogenic microorganisms (*P. aeruginosa* ATCC 27853, *E. coli*

ATCC 35218, *S. aureus* ATCC 12493, *S. aureus* (Mastitis isolate)) (Table 2). The results showed that the green-synthesized AgNPs exhibited antimicrobial activity at most concentrations tested, although the effect was not as strong as that of the positive control group using antibiotics. The antimicrobial activity of AgNPs was found to be proportional to the concentration of AgNPs in the solution. The highlighted point in this study is that the *S. aureus (Mastitis isolate)* strain group was found to be resistant to Tetracycline at 100 µg/l, but showed sensitivity to the antimicrobial activity of AgNPs at all studied concentrations (Figure 7). These results suggest that green-synthesized AgNPs may be a promising approach for addressing the global problem of antibiotic resistance. The ability of AgNPs to inhibit antibiotic-resistant strains of *S. aureus* is also consistently compared with previous studies, which have shown antibacterial effects against S. aureus or MRSA strains (Table 3).

3.6. The antifungal

The antifungal effect of synthesized AgNPs is shown in Figure 8. The fungal colony diameter of the AgNPs sample had significantly smaller fungal growth ring diameters than the negative control (sterilized distilled Water). Therefore, it demonstrates that AgNPs possess antifungal properties. The inhibition level of AgNPs at 200 ppm concentration against *Colletotrichum gloeopsoriodes* was 31.75%.

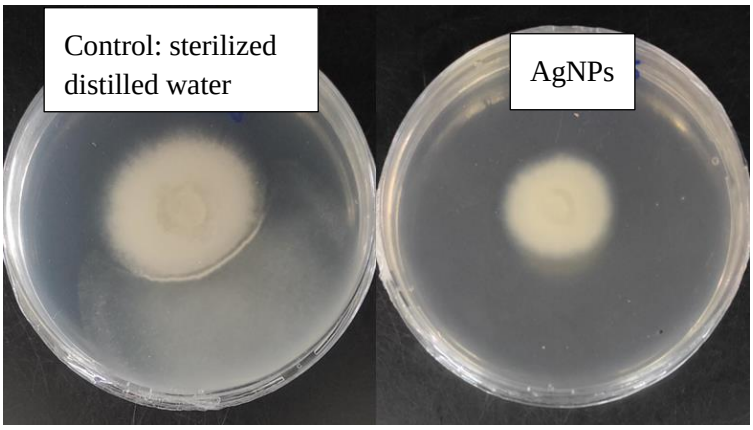

Figure 8. Antifungal activity of green synthesis of silver nanoparticles.

According to Dibrov *et al.* [41], silver nanoparticles have diameters ranging from 10 to 100 nm, enabling them to readily traverse the cell wall and access the cell membrane, thereby entering the cell. Such penetration is facilitated by the distinctive size effect and surface effect exhibited by these nanoparticles. The facile reactivity of AgNPs in cell solutions can be attributed to their substantial surface area. The oxidation half-reaction for silver (Ag) can be represented as $Ag = Ag^{+} + e^{-}$. Upon infiltration into the pathogen cell, the silver ion promptly binds to the sulfhydryl (–SH) group of the enzyme protein, rendering certain enzymes inactive. Consequently, the cell experiences a loss in its capacity to undergo division and reproduction.

4. CONCLUSIONS

In summary, an eco-friendly method was successfully employed for synthesizing silver nanoparticles (10 - 30 nm) using *S. nervosum* leaf extract. The silver nanoparticles exhibited

plasmon absorption at a wavelength of approximately 435 nm, as indicated by the peak in the absorption spectrum. Notably, these environmentally friendly synthesized AgNPs displayed remarkable antibacterial activity against both Gram-positive bacteria (*S. aureus*) and Gram-negative bacteria (*P. aeruginosa*, *E. coli*). Furthermore, the AgNPs demonstrated the ability to inhibit antibiotic-resistant strains of *S. aureus*, suggesting their potential application in biochemistry and offering new possibilities for alternative materials to replace antibiotics in the future.

Acknowledgements. The work received support from QTRU01.02/21-22 under the VAST grant.

Authors' contributions. Cong Hong Hanh: original draft, data collecting, experiment design, investigation, and data analysis. Tran Que Chi, Nguyen Hong Nhung, Nguyen Van Phuong: data collecting, investigation, and data analysis. Tran Thi Huong, Pham Thi Gam: Data analysis. Hoang Hien Y, Dao My Uyen, Phan Thi Thanh Nga: Methodology, Writing—review & editing. Pham Sy Hieu, Pham Duy Khanh: methodology, and Hoang Anh Son: supervision and conceptualization of the manuscript.

Declaration of competing interest. The authors declare that they have no known competing financial interests or personal relationships that could have appeared to influence the work reported in this paper.

REFERENCES

1. Jamkhande P. G., Ghule N. W., Bamer A. H., Kalaskar M. G. - Metal nanoparticles synthesis: An overview on methods of preparation, advantages and disadvantages, and applications, Journal of Drug delivery Science and Technology **53** (2019) 101174.
2. Ingle A. P., Duran N., Rai M. - Bioactivity, mechanism of action, and cytotoxicity of copper-based nanoparticles: a review, Applied microbiology and Biotechnology **98** (2014) 1001-1009.
3. Wu B., Kuang Y., Zhang X., Chen J. - Noble metal nanoparticles/carbon nanotubes nanohybrids: synthesis and applications, Nano Today **6** (1) (2011) 75-90.
4. Zhang F., Zhu Y., Lin Q., Zhang L., Zhang X., Wang H. - Noble-metal single-atoms in thermocatalysis, electrocatalysis, and photocatalysis, Energy & Environmental Science **14** (5) (2021) 2954-3009.
5. Klębowski B., Depciuch J., Parlinska-Wojtan M., Baran J. - Applications of noble metal-based nanoparticles in medicine, International Journal of Molecular Sciences **19** (12) (2018) 4031.
6. Doria G., Conde J., Veigas B., Giestas L., Almeida C., Assunção M., Rosa J., Baptista P. V. - Noble metal nanoparticles for biosensing applications, Sensors **12** (2) (2012) 1657-1687.
7. Yang T. H., Ahn J., Shi S., Wang P., Gao R., Qin D. - Noble-metal nanoframes and their catalytic applications, Chemical Reviews **121** (2) (2020) 796-833.
8. Emam H. E., El-Zawahry M. M., Ahmed H. B. - One-pot fabrication of agnps, aunps and ag-au nanoalloy using cellulosic solid support for catalytic reduction application, Carbohydrate polymers **166** (2017) 1-13.
9. Qu J. C., Ren C. L., Dong Y. L., Chang Y. P., Zhou M., Chen X. G. - Facile synthesis of multifunctional graphene oxide/agnps-fe3o4 nanocomposite: A highly integrated catalysts, Chemical engineering journal **211** (2012) 412-420.
10. Yang J., Chen Y., Zhao L., Feng Z., Peng K., Wei A., Wang Y., Tong Z., Cheng B. - Preparation of a chitosan/carboxymethyl chitosan/AgNPs polyelectrolyte composite

physical hydrogel with self-healing ability, antibacterial properties, and good biosafety simultaneously, and its application as a wound dressing, Composites Part B: Engineering **197** (2020) 108139.

11. Yang Y., Zhang C., Hu Z. - Impact of metallic and metal oxide nanoparticles on wastewater treatment and anaerobic digestion, Environmental Science: Processes & Impacts **15** (1) (2013) 39-48.
12. Singh S., Bharti A., Meena V. K. - Structural, thermal, zeta potential and electrical properties of disaccharide reduced silver nanoparticles, Journal of Materials Science: Materials in Electronics **25** (2014) 3747-3752.
13. Herrera-Marin P., Fernandez L., Pilaquinga F., Debut A., Rodriguez A., Espinoza-Montero P. - Green synthesis of silver nanoparticles using aqueous extract of the leaves of fine aroma cocoa theobroma cacao linneu (malvaceae): Optimization by electrochemical techniques, Electrochimica Acta (2023) 142122.
14. Wei L., Lu J., X. H., Patel A., Chen Z. S., Chen G. - Silver nanoparticles: synthesis, properties, and therapeutic applications. Drug discovery today **20** (5) (2015) 595-601.
15. Thi H. P. N., Thi K. T. P., Nguyen T. T., Nguyen P. T., Vu T. T., Le H. T., Dang T. D., Huynh D. C., Mai H. T., La D.D ., *et al.* - Green synthesis of an Ag nanoparticle-decorated graphene nanoplatelet nanocomposite by using cleistocalyx operculatus leaf extract for antibacterial applications, NanoStructures & Nano-Objects **29** (2022) 100810.
16. Pourzahedi L., Eckelman M. J. - Comparative life cycle assessment of silver nanoparticle synthesis routes, Environmental Science: Nano **2** (4) (2015) 361-369.
17. Kapoor R. T., Salvadori M. R., Rafatullah M., Siddiqui M. R., Khan M. A., Alshareef S. A. - Exploration of microbial factories for synthesis of nanoparticles–a sustainable approach for bioremediation of environmental contaminants, Frontiers in Microbiology **12** (2021) 658294.
18. Ahmed S. F., Mofijur M., Rafa N., Chowdhury A. T., Chowdhury S., Nahrin M., Islam A. S., Ong H. C. - Green approaches in synthesising nanomaterials for environmental nanobioremediation: Technological advancements, applications, benefits and challenges, Environmental Research **204** (2022) 111967.
19. Bharadwaj K. K., Rabha B., Pati S., Sarkar T., Choudhury B. K., Barman A., Bhattacharjya D., Srivastava A., Baishya D., Edinur H.A., *et al*. - Green synthesis of gold nanoparticles using plant extracts as beneficial prospect for cancer theranostics, Molecules **26** (21) (2021), 6389.
20. Kuppusamy P., Yusoff M. M., Maniam G. P., Govindan N. - Biosynthesis of metallic nanoparticles using plant derivatives and their new avenues in pharmacological applications–an updated report, Saudi Pharmaceutical Journal **24** (4) (2016) 473-484.
21. Jalab J., Abdelwahed W., Kitaz A., Al-Kayali R. - Green synthesis of silver nanoparticles using aqueous extract of acacia cyanophylla and its antibacterial activity, Heliyon **7** (9) (2021) 08033.
22. Guimaraes M. L., Silva F. A. G., Costa M. M., Oliveira H. P. - Green synthesis of silver nanoparticles using ziziphus joazeiro leaf extract for production of antibacterial agents, Applied Nanoscience **10** (2020) 1073-1081.
23. Pham G. N., Nguyen T. T. T., Nguyen-Ngoc H. - Ethnopharmacology, phytochemistry, and pharmacology of *Syzygium nervosum*, Evidence-Based Complementary and Alternative Medicine **2020** (2020) eCollection. DOI 10.1155/2020/8263670.

24. Nguyen T. H. P., Pham T. K. T., Nguyen T. L., *et al*. - Green synthesis of an Ag nanoparticle-decorated graphene nanoplatelet nanocomposite by using Cleistocalyx operculatus leaf extract for antibacterial applications, Nanostructures & Nano-Objects **29** (2022) 100810.
25. Bruna T., Maldonado-Bravo F., Jara P., and Caro N. - Silver nanoparticles and their antibacterial applications, Int. J. Mol. Sci. **22** (13) (2021) 7202.
26. Cheng G., Dai M., Ahmed S., *et al*. - Antimicrobial drugs in fighting against antimicrobial resistance.,Front. Microbiol. **7** (2016) 470. doi: 10.3389/fmicb.2016.00470.
27. Balouiri M., Sadiki M., Ibnsouda S. K. - Methods for in vitro evaluating antimicrobial activity: A review, Journal of pharmaceutical analysis **6** (2) (2016) 71-79.
28. Magaldi S., Mata-Essayag S., De Capriles C. H., Pérez C., Colella M., Olaizola C., Ontiveros Y. - Well diffusion for antifungal susceptibility testing, International Journal of Infectious Diseases **8** (1) (2004) 39-45.
29. Wollenberg R. D., Donau S. S., Nielsen T. T., Sørensen J. L., Giese H., Wimmer R., Søndergaard T. E. - Real-time imaging of the growth-inhibitory effect of JS399-19 on Fusarium, Pesticide Biochemistry and Physiology **134** (2016) 24-30.
30. Kim S. W., Jung J. H., Lamsal K., Kim Y. S., Min J. S., Lee Y. S. - Antifungal effects of silver nanoparticles (AgNPs) against various plant pathogenic fungi, Mycobiology **40** (1) (2012) 53-58.
31. Hu M., Novo C., Funston A., Wang H., Staleva H., Zou S., Mulvaney P., Xia Y., Hartland G. V. - Dark-field microscopy studies of single metal nanoparticles: understanding the factors that influence the linewidth of the localized surface plasmon resonance, Journal of materials chemistry **18** (17) (2008) 1949-1960.
32. Venkatesham M., Ayodhya D., Madhusudhan A., Veera Babu N., Veerabhadram G. - A novel green one-step synthesis of silver nanoparticles using chitosan: catalytic activity and antimicrobial studies. Applied Nanoscience **4** (2014) 113–119.
33. Hanafiah R.M., Ghafar S.A.A., Lim V., Musa S.N.A., Yakop F., Anuar A.H.H.– Green synthesis, characterisation and antibacterial activities of *Strobilanthes crispus* - mediated silver nanoparticles (SC-AGNPS) against selected bacteria, Artificial Cells, Nanomedicine, and Biotechnology **51** (1) (2023) 549-559.
34. Yusuf S. N. A. M., Mood C. N. A. C., Ahmad N. H. - Optimization of biogenic synthesis of silver nanoparticles from flavonoid-rich *Chinacanthus nutans* leaf and stem aqueous extracts, R. Soc. Open Sci. **7** (2020) 200065.
35. Parthipan P., AlSalhi M. S., Devanesan S., Rajasekar A. - Evaluation of *Syzygium aromaticum* aqueous extract as an eco-friendly inhibitor for microbiologically influenced corrosion of carbon steel in oil reservoir environment, Bioprocess and Biosystems Engineering **44** (2021) 1441-1452.
36. Chand K., Abro M. I., Aftab U., Shah A. H., Lakhan M. N., Cao D., Mehdi G., Mohamed A. M. A. - Green synthesis characterization and antimicrobial activity against staphylococcus aureus of silver nanoparticles using extracts of neem, onion and tomato, RSC advances **9** (30) (2019) 17002-17015.
37. Saadh M. - Effect of silver nanoparticles on the antibacterial activity of Levofloxacin against methicillinresistant staphylococcus aureus, Eur. Rev. Med. Pharmacol. Sci **25** (17) (2021) 5507-5510.

38. Salah R., Karmy M., Abdelraouf A., Kotb S. - Evaluation of the bactericidal effect of silver nanoparticles against methicillin resistant *staphylococcus aureus* (MRSA) and methicillin sensitive *staphylococcus aureus* (MSSA) strains isolated from mastitic milk of small ruminants and their surrounding environment in Aswan, Egypt, Journal of Veterinary Medical Research **27** (2) (2020) 143-151.
39. Mirzajani F., Ghassempour A., Aliahmadi A., Esmaeili M. A. - Antibacterial effect of silver nanoparticles on *Staphylococcus aureus*, Research in microbiology **162** (5) (2011) 542-549.
40. Qasim M., Udomluck N., Chang J., Park H., Kim K. - Antimicrobial activity of silver nanoparticles encapsulated in poly-n-isopropylacrylamide-based polymeric nanoparticles, International journal of nanomedicine **13** (2018) 235.
41. Dibrov P., Dzioba J., Gosink K.K., Hase C. C. - Chemiosmotic mechanism of antimicrobial activity of Ag+ in *vibrio cholerae*, Antimicrobial agents and chemotherapy **46** (8) (2022) 2668-2670.